

Published in final edited form as:

J Mol Neurosci. 2012 July ; 47(3): 631–638. doi:10.1007/s12031-011-9699-8.

Proximal giant neurofilamentous axonopathy in mice genetically engineered to resist calpain and caspase cleavage of α -2 spectrin

R. Kassa¹, V. Monterroso², J. Wentzell¹, A.L. Ramos¹, E. Couchi⁵, MC Lecomte⁶, M Iordanov⁴, D. Kretzschmar¹, G. Nicolas⁷, and D. Tshala-Katumbay^{1,3}

¹Center for Research on Occupational and Environmental Toxicology, Oregon Health & Science University (OHSU), Portland, OR, USA

²Department of Comparative Medicine, Oregon Health & Science University (OHSU), Portland, OR, USA

³Department of Neurology, Oregon Health & Science University (OHSU), Portland, OR, USA

⁴Department of Cell and Developmental Biology, Oregon Health & Science University (OHSU), Portland, OR, USA

⁵UFR de Médecine site Bichat, Institut Claude Bernard, Université Paris Diderot, Paris 7, France

⁶INSERM, U665, Paris; Institut National de la Transfusion Sanguine, Paris, F-75015; Université Denis Diderot, Paris 7, France

⁷Institut Cochin, Université Paris-Descartes, CNRS (UMR 8104) & INSERM, U1016, Paris, France

Abstract

We use 1,2-diacetylbenzene (1,2-DAB) to probe molecular mechanisms of proximal giant neurofilamentous axonopathy (PGNA), a pathological hallmark of amyotrophic lateral sclerosis. The spinal cord proteome of rodents displaying 1,2-DAB-PGNA suggests a reduction in the abundance of α II-spectrin (Spna2), a key protein in the maintenance of axonal integrity. Protein immunoblotting indicates that this reduction is due Spna2 degradation. We investigated the importance of such degradation in 1,2-DAB-PGNA. Spna2 mutant mice lacking a calpain- and/or caspase-sensitive domain (CSD), thus hypothetically resistant to 1,2-DAB, and wild-type littermates, were treated with 1,2-DAB, 35 mg/kg/day, or saline-control, for 3 weeks. 1,2-DAB induced motor weakness and PGNA irrespective of the genotype. Spna2-calpain breakdown products were not detected in mutant mice, which displayed a normal structure of the nervous system under saline-treatment. Intriguingly, treatment with 1,2-DAB reduced the abundance of the caspase-specific 120 kDa Spna2 breakdown products. Our findings indicate that degradation of Spna2 by calpain- and/or caspase is not central to the pathogenesis of 1,2-DAB axonopathy. In addition, the Spna2-CSD seems to be not required for the maintenance of the cytoskeleton integrity. Our conceptual framework offers opportunities to study the role of calpain-caspase cross-talk, including that of the protease degradomics, in models of axonal degeneration.

Corresponding author: Desire D. Tshala-Katumbay, MD, PhD, Center for Research on Occupational and Environmental Toxicology, Oregon Health & Science University, 3181 Sam Jackson Park Road, Mail code L606, Portland OR 97239 USA, Phone:

+1-503-494-0999; Fax: +1-503-494-6831; tshalad@ohsu.edu.

*The first two authors have equally contributed to the study.

Keywords

1,2-diacetylbenzene; α II-spectrin; calpain; caspase; neurodegeneration

Introduction

Proximal giant neurofilamentous axonopathy (PGNA) is an early pathological hallmark of a host of neurodegenerative diseases, including the amyotrophic lateral sclerosis, of which the pathogenetic mechanisms remained unclear. Giant axons filled with 10nm-neurofilaments (NF) mostly develop at proximal sites of elongated motor axons (Delisle and Carpenter, 1984; Hirano et al., 1984; Okamoto et al., 1990; Al-Chalabi and Miller, 2003). These sites are enriched with the structural protein α -II spectrin (Spna2), reportedly critical for the neurobiology of axon pathfinding, neuronal plasticity, and maintenance of the cytoskeleton integrity through cycles of calpain- and caspase-mediated proteolysis (Simonovic et al., 2006; Meary et al., 2007). The role of such physiological process in response to neurodegenerative stimuli has yet to be elucidated.

We use 1,2-diacetylbenzene (1,2-DAB), a γ -diketone-like neuroprotein-reactant as probe to study molecular mechanisms associated with PGNA (Tshala-Katumbay et al., 2005, 2008, and 2009). Two-dimensional differential in-gel electrophoresis (2D-DIGE) in combination with matrix-assisted laser desorption time-of-flight tandem mass spectrometry (MALDI-TOF/MS-MS) have shown that Spna2 was a target of 2,5-hexanedione (2,5-HD), the neurotoxic aliphatic cousin of 1,2-DAB (Tshala-Katumbay et al., 2009; Spencer et al., 2002). Protein immunoblots of tissues from animals treated with the aforementioned neurotoxic compounds, at doses that induce comparable neuromuscular weakness (Conference proceedings, IXth meeting of the International Neurotoxicology Association, Germany, 2003), showed that Spna2 was cleaved through a proteolytic pattern consistent with the activation of calpains and/or caspases (Meary et al., 2007). Both γ -diketones look-alike 1,2-DAB and 2,5-HD crosslink neuroproteins and induce axonal damage by mechanisms that have yet to be elucidated (Spencer et al., 2002). In this study, we asked whether the proteolysis, mainly calpain- and/or caspase-mediated, of Spna2 was central to the development of the PGNA seen in animals treated with the 1,2-DAB. Mutant Spna2^{tm1.1Gnic} mice that lack a domain sensitive to proteases calpains and/or caspases (CSD) of Spna2, but possibly sensitive to yet not elucidated caspase-proteolytic mechanisms (Wang, 2000; Warren et al., 2005; Meary et al., 2007), and their wild type (WT) littermates, were treated with 1,2-DAB, 35 mg/kg/day, or equivalent amount of 1,2-DAB-vehicle control, 5 days a week, for 3 weeks.

Control Spna2^{tm1.1Gnic} mice and their WT littermates displayed a normal phenotype and structure of peripheral nerves. However, those treated with 1,2-DAB displayed motor weakness and intraspinal 10nm-NF filled axonal swellings. Intriguingly, calpain- and caspase-specific proteolytic mechanisms (associated with the 120kDa breakdown product of Spna2) showed a differential pattern of susceptibility to 1,2-DAB; a pattern that was seen in animals with end-stage severe motor weakness. These findings indicate that degradation of Spna2 by calpains and/or caspases may not be central to the pathogenesis of 1,2-DAB-induced PGNA. In addition, they suggest that the CSD of Spna2 may not be relevant for the maintenance of the cytoskeleton integrity in peripheral nerves. Our experimental framework offers opportunities for studies that may further elucidate the role of calpain-caspase cross-talk, including that of the protease degradomics, in models of axonal degeneration (Zhao et al., 1999; Wang, 2000; Robert et al., 2002; Overall et al., 2004; Warren et al., 2005 and 2007).

Materials and Methods

Chemicals

1,2-DAB (99%) was purchased from Aldrich Chemical Co. (Madison, WI) and desiccated at room temperature. The stock sample was checked by gas chromatography-mass spectrometry to confirm the purity of the chemical.

Animals

Heterozygous *Spna2*^{Δm1.1Gnic} mice backcrossed nine times on C57BL/6 background were kindly provided by Dr. Nicolas, INSERM (Institut National de la Santé et de la Recherche Médicale, France). In these mice, the three exons in *Spna2* encoding the calmodulin binding domain, and the caspase- and calpain-cleavage sites, were deleted using a classical knockout approach while keeping the rest of the encoded mutant *Spna2* intact so as not to impair the translation reading frame (Meary et al, 2007). A mutant colony was established in our institute (Department of Comparative Medicine) by interbreeding heterozygous mice. Animals, including the WT littermates of *Spna2* mutants, were kept on 12-h/12-h light dark cycle, and food and water were given *ad libitum*. Studies were conducted in accordance with the institutional (OHSU) guidelines for the care and use of laboratory animals.

Genotyping

Two-5mm long tail biopsy specimen were taken from 14–21 days old mice for genotyping. To extract DNA, tail biopsies were digested overnight at 55°C in 200 μl of 1 mg/ml proteinase-K in 100 mM Tris (pH 8.5), 5 mM EDTA, 200 mM NaCl buffer. Afterwards, digest samples were boiled for 15 min to inactivate proteinase K and then DNA ethanol precipitated. Genomic DNA (1–2 μl) was used in a 25 μl multiplex polymerase chain reaction (PCR) that included the following primers: primer 1, forward 5'-gatctgaaagccaatgagtctcggc-3'; primer 2, forward 5'-tacatagagaatggccagctctttgac-3'; and primer 3, reverse 5'-gcacaactgggtaaggttaaggttctattcc-3'. The PCR mix consisted of 20 mM Tris HCl (pH 8.4), 50 mM KCl, 2 mM MgCl₂, 0.2 mM dNTPs, 0.18 mM primers 1–3, and 0.5 unit Taq polymerase (Invitrogen, Carlsbad, CA). After an initial denaturation at 94°C for 4 min, 35 cycles of 20 sec at 94°C, 20 sec at 65°C, and 30 sec at 72°C were carried out followed by a final elongation at 72°C for 5 min. PCR products were separated by electrophoresis through a 2% agarose gel containing SYBR safe (Invitrogen, Carlsbad, CA). The WT *Spna2* allele amplified a single 201 base pairs (bp) amplicon with primers 2+3. The mutant *Spna2* allele amplified single 374 bp amplicon with primers 1+3. Heterozygous animals showed both 201 bp and 374 bp amplicons. Regular genotyping of new progeny for our heterozygous-based breeding colony revealed animals with expected genotypes; with amplicon bands corresponding to the expected lengths of *Spna2*.

Animal treatment, observation and motor tests

Young adult male mice (homozygous *Spna2*^{Δm1.1Gnic} or their WT littermates, n = 10 per genotype) were treated intraperitoneally (i.p.) with 1,2-DAB at a dose of 35 mg/kg body weight/day (n=7/genotype/study 1 & 2), or equivalent amount of vehicle (2% acetone in 0.9% saline; n=3–4/genotype/study 1 & 2), once daily, 5 days a week, for 3 weeks. This dosing schedule was previously used to develop the mouse model for 1,2-DAB axonopathy (Tshala-Katumbay et al., 2005) and conduct preliminary studies in the *Spna2* mutant (study 1) prior to the formal experiment (study 2). During both studies, injection sites were rotated around the abdomen and care was taken to minimize leakage and discomfort.

Animals were weighed daily to check for changes in body weight and adjustment of the 1,2-DAB dose. They were also examined daily for the presence of the hindlimb extension reflex, elicited when the animal is gently raised by the tail. In addition, mice were assessed for

deficits in motor coordination using a software-driven rotarod apparatus (AccuScan Instruments, Inc., Columbus, OH). Animals were placed on a rotating rod (70-mm diameter) in a constant mode set at 7 rpm. The apparatus had an automatic fall detection system comprising photobeams. Animals were tested 3 times a week with 2 consecutive trials per session and a cutoff point of 180 sec. The latency to fall was measured during each trial.

Animal perfusion and tissue processing protocols

At study termination, animals that have developed severe motor weakness were deeply anesthetized with 4% isoflurane (1 l oxygen/min). Those retained for biochemical studies were transcardially perfused with 0.01M phosphate-buffered saline (PBS, pH 7.4) to remove blood. Immediately thereafter, the spinal cord was removed by pressurized saline extrusion. Lumbosacral spinal cord segments were flash-frozen in liquid nitrogen and stored at -80°C for Western blotting studies.

For ultrastructural studies, animals were transcardially perfused with PBS followed by 4% paraformaldehyde and 5% glutaraldehyde in 0.1M sodium cacodylate buffer (pH 7.4). The lumbosacral segment of the spinal cord, and the proximal sciatic nerves from both sides were dissected out, postfixed in 1% osmium tetroxide in PBS, dehydrated and embedded in epoxy resin. Cross-sections (~ 900 nm) of fixed tissue were stained with 1% toluidine blue and screened by bright-field microscopy. Thin sections (~ 90 nm) of regions of interest were stained with 2% uranyl acetate followed by 1% lead citrate and examined by transmission electron microscopy (TEM).

Western blotting

Spinal cord tissues were subjected to direct ultrasonic shearing in 2X sodium dodecyl sulfate polyacrylamide gel electrophoresis sample-loading buffer, followed by heat denaturation at 95°C for 5 min. One hundred μg wet tissue were homogenized in 0.1 ml of buffer per mg. Tissue lysates were stored at -70°C until later use for protein immunoblotting as previously described (Banay-Schwartz et al, 1992). Proteins were resolved by 7.5% sodium dodecyl sulfate polyacrylamide gels and transferred overnight to polyvinylidene difluoride membranes (Millipore, Billerica, MA). Loading variations were ruled out after protein immunoblots using the glucosidase-2 β (Gl-II β) antibody (Santa Cruz Biotechnology, CA). Membranes were incubated with 10% dry milk in Tris-buffered saline containing 0.3% Tween-20 (TBST) for 0.5 h to block non-specific binding and immunoprobed for 1 h at room temperature with the mouse monoclonal antibody to Spna2 (clone AA6 from Enzo Life Sciences, Plymouth Meeting, PA; dilution 1:1000 in 5% dry milk/TBST). After incubation with a goat anti-mouse horseradish peroxidase-conjugated antibody (Santa Cruz Biotechnology; 1:2000 in 5% dry milk/TBST), peroxidase activity was detected with an enhanced chemiluminescent detection system (DuPont NEN Research Products, Boston, MA) following the manufacturer's instructions.

Statistical analysis

A linear contrast was computed for each animal's weekly series of body weight measurements, resulting in three contrasts per animal, with each contrast interpretable as the average change in body weight per day. The collection of three contrasts was then analyzed using multivariate analysis of variance to determine whether the daily average change in body weight was influenced by treatment, genotype, or the interaction between these factors.

The mean latency to fall from the rotarod for each genotype and treatment-based group (i.e., WT vehicle, WT 1,2-DAB, mutant vehicle, and mutant 1,2-DAB) was computed for each rotarod session, resulting in three mean values per week. The between group difference in

these values (mean latency to fall from rotarod/day/group) for each week was then analyzed with 2-way analysis of variance (ANOVA).

Densitometric analysis of the Gl-II β -standardized intensity of bands corresponding to 280 (mutant) or 285 (WT) full-length Spna2, or 150- and 120-kDa spectrin breakdown products (SBDP), was done on digitized Western blot images using the Image J software from the National Institute of Health (NIH). The between group difference in the mean gray values of the 280/285-kDa bands, and ratio of the mean gray values of 120-kDa SBDP bands vs. their corresponding 280- or 285-kDa bands was evaluated with 2-way ANOVA; and the ratio of the mean gray values of the 150- vs. 285-kDa bands analyzed with one-way ANOVA. Differences were considered statistically significant at $p < 0.05$.

Results

Body weight, motor signs, and rotarod performance

Vehicle-injected WT and mutant mice showed no significant changes in body weight. 1,2-DAB-treated animals lost an average of 0.44 grams/day (95% confidence interval (CI): 0.31–0.58 grams/day) during the first week regardless of the genotype. During the second and third week, the loss in body weight averaged 0.82 grams/day (95% CI: 0.71–0.92 grams/day). Neither the Spna2 mutant mice nor the WT mice injected with vehicle showed abnormalities in locomotion and performed equally well on the rotarod apparatus. Animals treated with 1,2-DAB exhibited gait abnormalities after the first week of treatment. Similar motor deficits were seen in the Spna2 mutant mice. Both genotypes showed a hunched-back posture, a broad-based gait, and dragged all four limbs by the end of the study. In addition, a progressive decrease in latency to fall from the rotating rod was found in 1,2-DAB-treated animals from the second week onwards compared to the vehicle-injected, and genotype did not modify the effect of 1,2-DAB on rotarod performance (mean latency to fall/treatment group \pm standard error of the mean: 180 ± 14 sec for vehicle-treated animals vs. 112 ± 19 sec for 1,2-DAB-treated animals during week 2, $p < 0.05$; or 180 ± 14 sec vs. 67 ± 14 sec for vehicle- vs. 1,2-DAB-treated animals, respectively, during Week 3, $p < 0.0001$).

Western blotting

We performed a Western blotting analysis of spinal cord homogenates to determine the effect of 1,2-DAB treatment on Spna2 cleavage in mutants compared to WT mice. After controlling for loading variations, no statistical difference in the immunosignal intensity of the full-length bands was detected in 1,2-DAB-treated animals compared to vehicle-injected controls across the genotypes. Our statistical analyzes were conducted using means and/or ratios of densitometric values within genotypes. As expected, in Spna2 mutant mice, the 150 kDa SBDP were not detected. However, a significant increase in the mean relative abundance of this breakdown product was found in 1,2-DAB-treated WT animals compared to vehicle-injected WT ($p < 0.005$). A significant reduction in the relative abundance of the 120 kDa caspase-specific SBDP was found in 1,2-DAB-treated mice compared to vehicle-injected respective controls irrespective of the genotype ($p < 0.05$; Fig. 1).

Neuropathology

WT and mutant mice treated with vehicle retained a normal morphology of the spinal cord and proximal sciatic nerves. However, those treated with 1,2-DAB showed a bluish discoloration of tissues, and TEM structural abnormalities in the nervous system. In agreement with findings from motor assessment, no differences were detected in the neuropathological features induced by 1,2-DAB in Spna2 mice relative to WT animals. In both genotypes, examination of toluidine blue-stained lumbar spinal cord sections from both

WT and Spna2 mutant mice treated with 1,2-DAB showed enlarged 10nm-NF filled axons in lumbar anterior horns (Fig. 2 and 3).

Ultrastructural studies of the intraspinal swollen axons of 1,2-DAB-treated animals revealed axons densely-packed with maloriented 10nm-NF irrespective of the genotype. TEM of proximal sciatic nerves showed similar findings in addition to a clustering of microtubules and organelles (mitochondria) in both wild-type (Fig. 4) and mutant mice (Fig. 5).

Discussion

We report for the first time neuropathological changes induced by axonopathic 1,2-DAB in mutant mice genetically engineered to resist calpain and caspase cleavage of Spna2 (Meary et al., 2007). 1,2-DAB induces a bluish discoloration of nervous system tissues, motor weakness, and a PGNA in elongated motor axons irrespective of the mouse genotype. These findings remain consistent with those previously in rodents treated with 1,2-BAB (Kim et al., 2001; Spencer et al., 2002; Tshala-Katumbay et al., 2005). As expected, the 150 kDa breakdown products of Spna2 were not detected in mutant mice, which still displayed a normal phenotype and structure of peripheral sciatic nerves with and without vehicle-treatment. Intriguingly, treatment with 1,2-DAB reduced the expression of the 120 kDa caspase-specific SBDP even in the wild-type mice.

Changes in the expression of Spna2, including its proteolytic cleavage, have been linked to both normal physiological processes (Lynch and Baudry, 1987; Sikorski et al., 2000; Czogalla et al., 2005; Susuki and Rasband, 2008) and neurological insults including those associated with neurodegeneration (Nath et al., 1996; Zhao et al., 1999; Pike et al., 2001; Siman et al., 2004; Warren et al., 2005 and 2007; Indraswari et al., 2009) or axonal disease induced by γ -diketone-like compounds including 2,5-hexadione (Genter et al., 1988; Tshala-Katumbay et al., 2008 and 2009). However, the role of Spna2 specific domains, notably its CSD domain, has not been elucidated in relation to the integrity of the cytoskeleton in peripheral nerves. Our study suggests that the Spna2 CSD domain may not be relevant for the maintenance of the cytoskeleton integrity both in normal and Spna2^{tm1.1Gnic} mutant mice. These findings appear to be consistent with previous reports that suggest that the CSD mutation in the Spna2^{tm1.1Gnic} mice affects only the fragility of Spna2 to proteases and not its ability to be incorporated into the membrane skeleton (Meary et al., 2007). The genetic deletion of the CSD of Spna2 does not protect against the axonopathic effects of 1,2-DAB suggesting that the cleavage of Spna2 may be a downstream event in the pathogenesis of 1,2-DAB-axonopathy. In this later event, protein adduction, crosslinkings, and polymerization, have been proposed as primary pathogenetic events, as similarly hypothesized for 2,5-HD-induced axonopathy (DeCaprio, 1987; DeCaprio et al., 1987; Spencer et al., 2002; LoPachin and DeCaprio, 2005). The extent to which cellular mechanisms of proteolysis may be involved has, however, yet to be elucidated (Tshala-Katumbay et al., 2008 and 2009).

The increased abundance of the putatively 150 kDa calpain-specific SBDP relative to those specific to caspase cleavage of Spna2, i.e. the 120 kDa SBDP, raises interesting questions. The increase of 150 kDa SBDP in WT mice treated with 1,2-DAB, with no decrease in the abundance of the full-length native Spna2, may possibly be explained by an increased *de novo* synthesis of Spna2 in reaction to the axonopathic stress induced by 1,2-DAB. This proposal is consistent with previous findings that showed an increase in the expression of Spna2 in models neurodegeneration, some of which may be associated with proteolytic breakdown of Spna2 (Siman et al., 2004; Indraswari et al., 2009). This proposal underscores, however, the non-quantitative value of proteomic methodologies such as those we

previously used to estimate changes in the expression of Spna2 following animal intoxication with axonopathic γ -diketones (Tshala-Katumbay et al., 2008 and 2009).

The presence of 120 kDa caspase SBDP in WT mice is consistent with the earlier proposal that suggests the existence of secondary sites for caspase-cleavage of Spna2 (Meary et al., 2007). However, the decrease in their abundance following treatment with 1,2-DAB is intriguing. It is possible that caspases or their related aforementioned low-molecular weight SBDP fragments have higher affinity for the neuroprotein crosslinking agent 1,2-DAB and hence, become adducted by 1,2-DAB and subsequently directed towards other proteolytic systems; or, for caspases, inactivated in their functions after adduction by 1,2-DAB.

Our study has shown that the CSD of Spna2 may not be relevant for the maintenance of the cytoskeleton integrity in peripheral nerves. In addition, genetic deletion of the CSD of Spna2 is not protective against the deleterious effects of axonopathic 1,2-DAB. However, the possible differential susceptibility of calpain- vs. caspase-related proteolytic mechanisms (associated with the 120 kDa SBDP) to the axonopathic 1,2-DAB demonstrates the usefulness of our model for studies aimed at elucidating to the role of calpain-caspase cross-talk, including that of the protease degradomics, in models of axonal degeneration (Zhao et al., 1999; Wang, 2000; Robert et al., 2002; Overall et al., 2004; Warren et al., 2005 and 2007). This proposal, however, bears some limitations as the 145 kDa calpain-specific SBDP were not readily identifiable during our experimentations (Zhang et al., 2003; Liu et al., 2006).

Acknowledgments

We thank Nicole Desmarais and Eli Magnum, OHSU, for her technical assistance. These studies were supported by the NS052183 grant from the NIH-National Institutes of Neurological Disorders and Stroke, Bethesda, MD.

References

- Al-Chalabi A, Miller CC. Neurofilaments and neurological disease. *Bioessays*. 2003; 25:346–355. [PubMed: 12655642]
- Banay-Schwartz M, Kenessey A, DeGuzman T, Lajtha A, Palkovits M. Protein content of various regions of rat brain and adult and aging human brain. *Age*. 1992; 15:51–54.
- Czogalla A, Sikorksi AF. Spectrin and calpain: a ‘target’ and a ‘sniper’ in the pathology of neuronal cells. *Cell Mol Life Sci*. 2005; 62:1913–1924. [PubMed: 15990959]
- DeCaprio AP. N-hexane neurotoxicity: a mechanism involving pyrrole adduct formation in axonal cytoskeletal protein. *Neurotoxicology*. 1987; 8:199–210. [PubMed: 3550536]
- DeCaprio AP, Jackowski SJ, Regan KA. Mechanism of formation and quantitation of imines, pyrroles, and stable nonpyrrole adducts in 2,5-hexanedione-treated protein. *Mol Pharmacol*. 1987; 32:542–548. [PubMed: 3312999]
- Delisle MB, Carpenter S. Neurofibrillary axonal swellings and amyotrophic lateral sclerosis. *J Neurol Sci*. 1984; 63:241–250. [PubMed: 6538591]
- Genter St Clair MB, Amarnath V, Moody MA, Anthony DC, Anderson CW, Graham DG. Pyrrole oxidation and protein cross-linking as necessary steps in the development of gamma-diketone neuropathy. *Chem Res Toxicol*. 1988; 1:179–185. [PubMed: 2979729]
- Hirano A, Donnenfeld H, Sasaki S, Nakano I. Fine structural observations of neurofilamentous changes in amyotrophic lateral sclerosis. *J Neuropathol Exp Neurol*. 1984; 43:461–470. [PubMed: 6540799]
- Indraswari F, Wong PT, Yap E, Ng YK, Dheen ST. Upregulation of Dpysl2 and Spna2 gene expression in the rat brain after ischemic stroke. *Neurochem Int*. 2009; 55(4):235–242. [PubMed: 19524114]

- Kim MS, Sabri MI, Miller VH, Kayton RJ, Dixon DA, Spencer PS. 1,2-diacetylbenzene, the neurotoxic metabolite of a chromogenic aromatic solvent, induces proximal axonopathy. *Toxicol Appl Pharmacol.* 2001; 177:121–131. [PubMed: 11740911]
- Liu MC, Akle V, Zheng W, Dave JR, Tortella FC, Hayes RL, Wang KK. Comparing calpain- and caspase-3-mediated degradation patterns in traumatic brain injury by differential proteome analysis. *Biochem J.* 2006; 394:715–725. [PubMed: 16351572]
- LoPachin RM, DeCaprio AP. Protein adduct formation as a molecular mechanism of neurotoxicity. *Toxicol Sci.* 2005; 86:214–225. [PubMed: 15901921]
- Lynch G, Baudry M. Brain spectrin, calpain and long-term changes in synaptic efficacy. *Brain Res Bull.* 1987; 18(6):809–815. [PubMed: 3040193]
- Meary F, Metral S, Ferreira C, Eladari D, Colin Y, Lecomte MC, Nicolas G. A mutant α II-spectrin designed to resist calpain and caspase cleavage questions the functional importance of this process *in vivo*. *J Biol Chem.* 2007; 282:14226–14237. [PubMed: 17374614]
- Nath R, Raser KJ, Stafford D, Hajimohammadreza I, Posner A, Allen H, Talanian RV, Yuen P, Gilbertsen RB, Wang KKW. Non-erythroid α -spectrin breakdown by calpain and interleukin 1β -converting-enzyme-like protease(s) in apoptotic cells: contributory roles of both protease families in neuronal apoptosis. *Biochem J.* 1996; 319:683–690. [PubMed: 8920967]
- Okamoto K, Hirai S, Shoji M, Senoh Y, Yamazaki T. Axonal swellings in the corticospinal tracts in amyotrophic lateral sclerosis. *Acta Neuropathol.* 1990; 80:222–226. [PubMed: 2202191]
- Overall CM, Tam EM, Kappelhoff R, Connor A, Ewart T, Morrison CJ, Puente X, López-Otín C, Seth A. Protease degradomics: mass spectrometry discovery of protease substrates and the CLIP-CHIP, a dedicated DNA microarray of all human proteases and inhibitors. *Biol Chem.* 2004; 385(6):493–504. [PubMed: 15255181]
- Pike BR, Flint J, Dutta S, Johnson E, Wang KKW, Hayes RL. Accumulation of non-erythroid α II-spectrin breakdown products in cerebrospinal fluid after traumatic brain injury in rats. *J Neurochem.* 2001; 78:1297–1306. [PubMed: 11579138]
- Robert, W Neumar; Xu, Y. Anne; Gada, Hemal; Guttmann, Rodney P.; Siman, Robert. Cross-talk between calpain and caspase proteolytic systems during neuronal apoptosis. *J Biol Chem.* 2002; 278(16):14162–14167.
- Sikorski AF, Sangerman J, Goodman SR, Critz SD. Spectrin (betaSpIIsigma1) is an essential component of synaptic transmission. *Brain Res.* 2000; 852:161–166. [PubMed: 10661507]
- Siman R, McIntosh TK, Soltesz KM, Chen Z, Neumar RW, Roberts VL. Proteins released from degenerating neurons are surrogate markers for acute brain damage. *Neurobiol Dis.* 2004; 16(2): 311–320. [PubMed: 15193288]
- Simonovic M, Zhang Z, Cianci CD, Steitz TA, Morrow JS. Structure of the calmodulin α II-spectrin complex provides insight into the regulation of cell plasticity. *J Biol Chem.* 2006; 281:34333–34340. [PubMed: 16945920]
- Spencer PS, Kim MS, Sabri MI. Aromatic as well as aliphatic hydrocarbon solvent axonopathy. *Int J Hyg Environ Health.* 2002; 205:131–136. [PubMed: 12018006]
- Susuki K, Rasband MN. Spectrin and ankyrin-based cytoskeletons at polarized domains in myelinated axons. *Exp Biol Med (Maywood).* 2008; 233:394–400. [PubMed: 18367627]
- Tshala-Katumbay DD, Palmer VS, Kayton RJ, Sabri MI, Spencer PS. A new murine model of giant proximal axonopathy. *Acta Neuropathol.* 2005; 109:405–410. [PubMed: 15759132]
- Tshala-Katumbay D, Monterroso V, Kayton R, Lasarev M, Sabri M, Spencer P. Probing mechanisms of axonopathy Part I: Protein targets of 1,2-diacetylbenzene, the neurotoxic metabolite of aromatic solvent 1,2-diethylbenzene. *Toxicol Sci.* 2008; 105:134–141. [PubMed: 18502740]
- Tshala-Katumbay D, Monterroso V, Kayton R, Lasarev M, Sabri M, Spencer P. Probing mechanisms of axonopathy. Part II: Protein targets of 2,5-hexanedione, the neurotoxic metabolite of the aliphatic solvent n-hexane. *Toxicol Sci.* 2009; 107:482–489. [PubMed: 19033394]
- Wang KKW. Calpain and caspase: can you tell the difference? *Trends Neurosci.* 2000; 23:20–26. [PubMed: 10631785]
- Warren MW, Kobeissy FH, Liu MC, Hayes RL, Gold MS, Wang KKW. Concurrent calpain and caspase-3 mediated proteolysis of α II-spectrin and tau in rat brain after methamphetamine

exposure: A similar profile to traumatic brain injury. *Life Sci.* 2005; 78:301–309. [PubMed: 16125733]

Warren MW, Zheng W, Kobeissy FH, Liu MC, Hayes RL, Gold MS, Lerner SF, Wang KKW. Calpain- and caspase-mediated α II-spectrin and tau proteolysis in rat cerebrocortical neuronal cultures after ecstasy or methamphetamine exposure. *Int J Neuropsychopharmacol.* 2007; 10:479–489. [PubMed: 16882358]

Zhang SX, Bondada V, Geddes JW. Evaluation of conditions for calpain inhibition in the rat spinal cord: effective postinjury inhibition with intraspinal MDL28170 microinjection. *J Neurotrauma.* 2003; 20(1):59–67. [PubMed: 12614588]

Zhao X, Pike BR, Newcomb JK, Wang KKW, Posmantur RM, Hayes RL. Maitotoxin induces calpain but not caspase-3 activation and necrotic cell death in primary septo-hippocampal cultures. *Neurochem Res.* 1999; 24:371–382. [PubMed: 10215511]

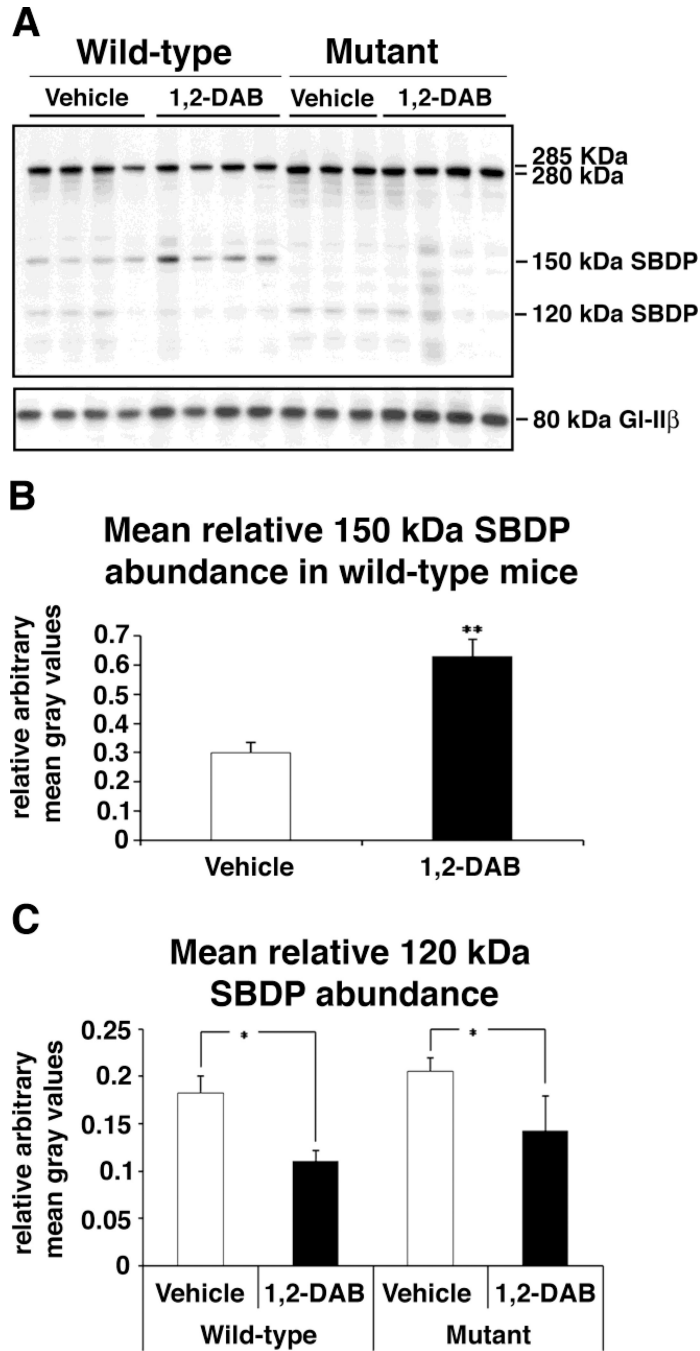


Figure 1.

(A). Left lanes: Spna2 immunoblots performed on spinal cord lysates from WT animals treated with vehicle or 1,2-DAB. The expression of the 150 kDa SBDP (Spna2 breakdown product) was increased in animals treated with 1,2-DAB. In contrast, the expression of the caspase specific 120 kDa SBDP seems to be decreased in animals treated with 1,2-DAB. Right lanes: Immunoblots for Spna2 mutant mice. Note the absence of the 150-kDa SBDP. A baseline expression of the 120 kDa SBDP in the vehicle-treated mice possibly occurs through a secondary Spna2 site for caspase-mediated proteolysis (Meary et al., 2007). GI-II β : loading control. (B) Densitometric evaluation of the immunosignal intensity of bands revealed a significant increase in the abundance (mean gray value \pm SD) of the 150-kDa

SBDP relative to that of the full-length 285-kDa Spna2 (** = $p < 0.005$). (C) Densitometric findings revealed a significant reduction in the abundance (mean gray value \pm SD) of the 120-kDa SBDP relative to that of the full-length Spna2 in both genotypes after treatment with 1,2-DAB (* = $p < 0.05$).

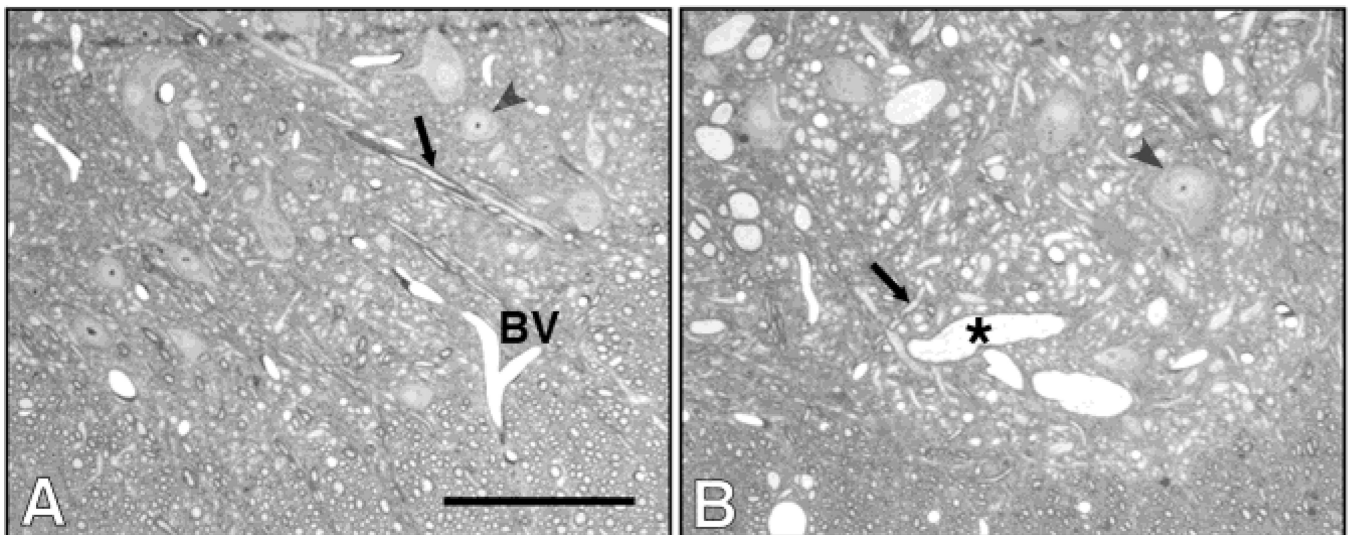


Figure 2. Cross sections of ventral horns in lumbar spinal cords from vehicle- (A) and 1,2-DAB-wild-type treated animals. Giant axonal swellings (*) were seen in lumbar anterior horns. Arrows: normal axons. Arrowheads: cell bodies. BV: blood vessel. Scale bar: 200 μ m.

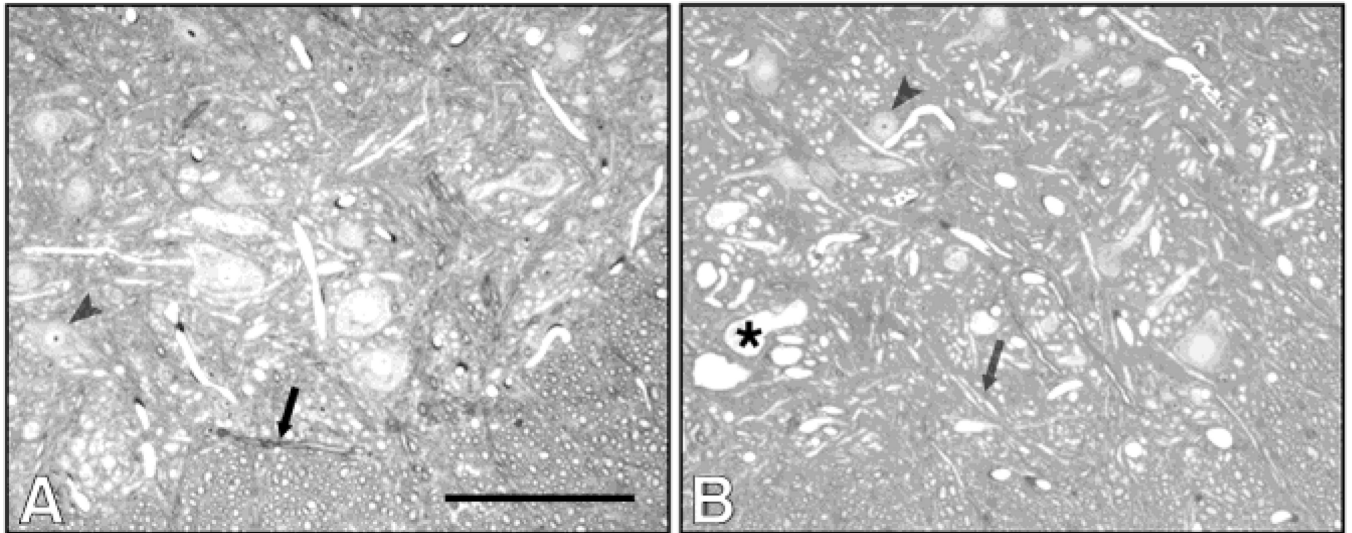


Figure 3.

Micrographs from *Spna2* mutants treated with vehicle (A) or 1,2-DAB (B). The anterior horns of these animals displayed a pathology similar to that seen in wild-type animals. Giant axonal swellings (*) were also seen in these animals, following treatment with 1,2-DAB. Arrows: normal axons. Arrowheads: cell bodies. BV: blood vessel. Scale bar: 200 μ m.

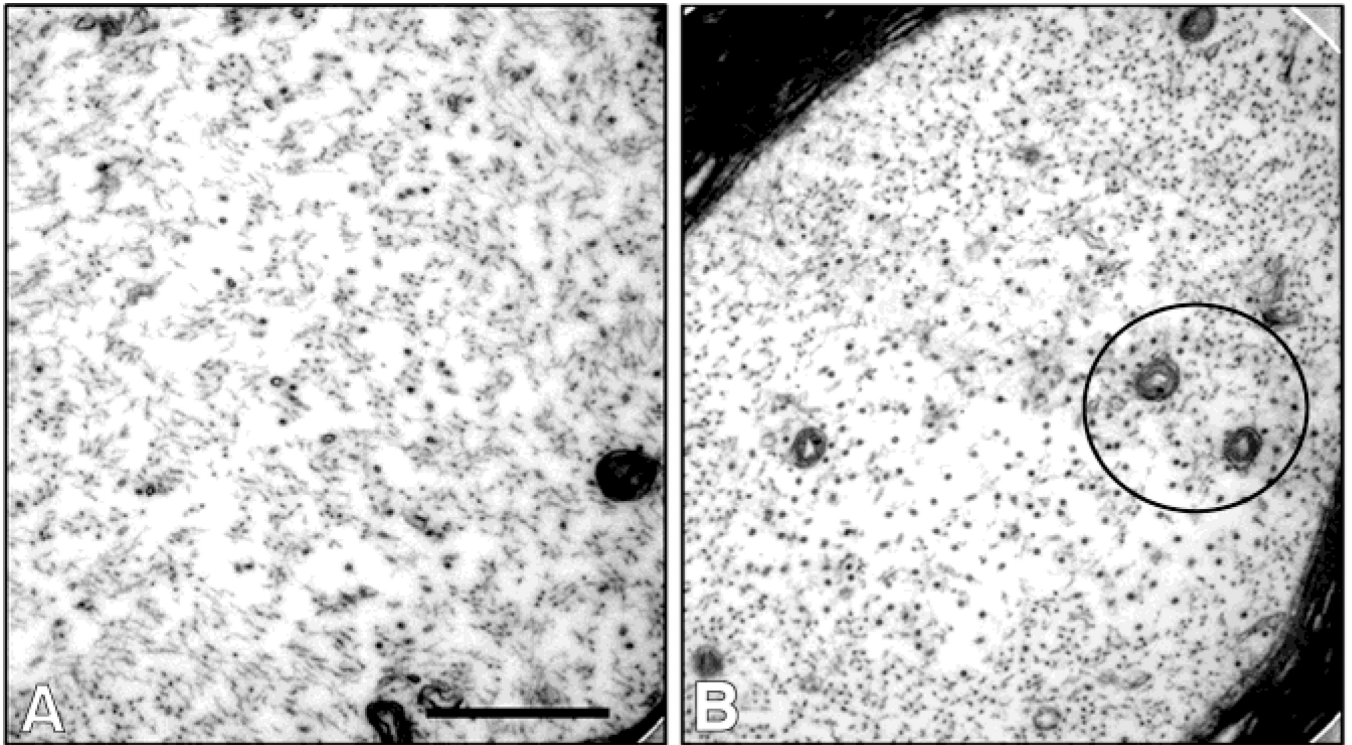


Figure 4. Transmission electron micrographs of sciatic nerves from vehicle- (A) or 1,2-DAB-treated wild-type mice. Densely packed axons and clustering of organelles and microtubules (circles) were seen in animals treated with 1,2-DAB (B) relative to vehicle-treated ones (A). Scale bar: 500 nm.

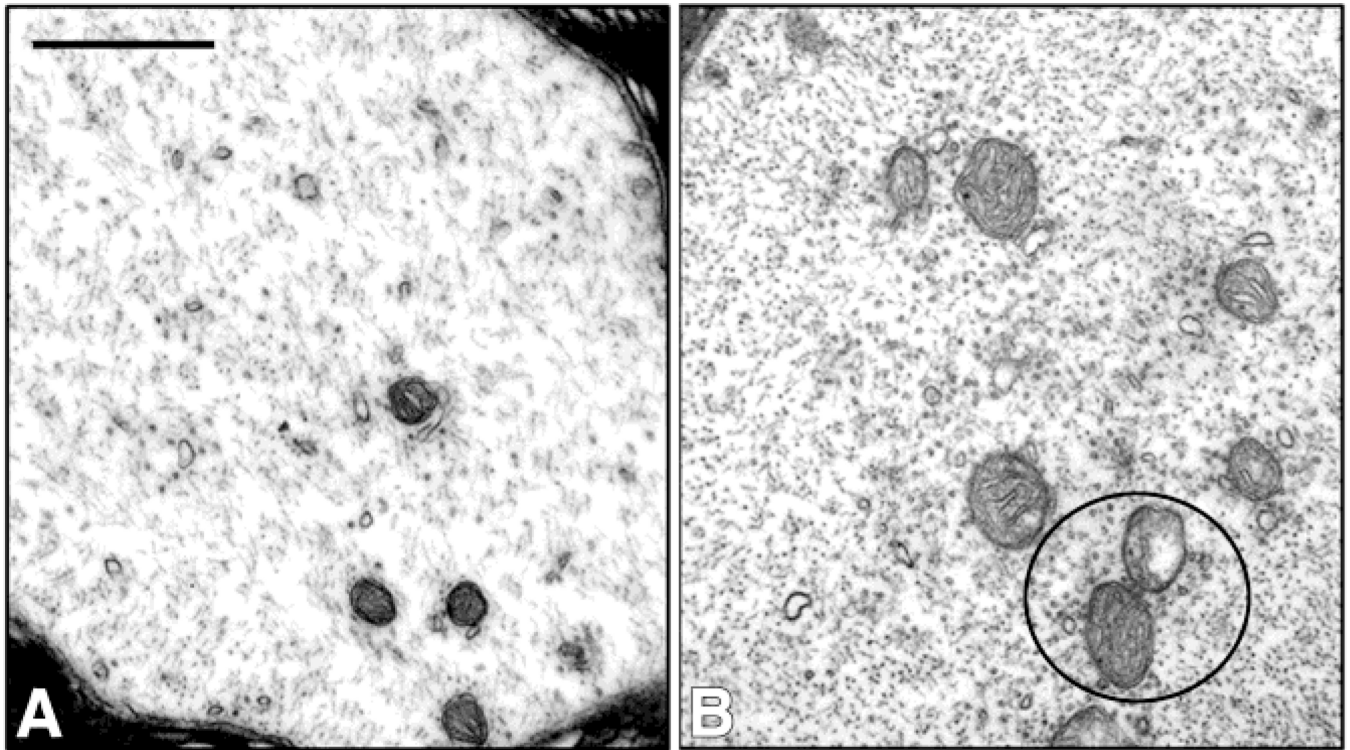


Figure 5. Micrographs from Spna2 mutants treated with vehicle (A) or 1,2-DAB- (B). Densely packed axons and clustering of organelles and microtubules (circles) were seen in 1,2-DAB-treated animals (B) relative to vehicle-treated ones (A). Scale bar: 500 nm.